Malaysian Journal of Analytical Sciences (MJAS)
Published by Malaysian Analytical Sciences Society

ENHANCING THE HYDROGEN GAS SENSING PROPERTIES OF ZINC OXIDE DOPED WITH ALUMINUM PREPARED VIA THERMAL OXIDATION

(Meningkatkan Sifat Penderiaan Gas Hidrogen bagi Zink Oksida Terdop Aluminium yang Disediakan dengan Kaedah Pengoksidaan Terma)

Naif H. Al-Hardan[1*], Muhammad Azmi Abdul Hamid[1], Azlan Abdul Aziz[2], Naser M. Ahmed[2]

[1]Department of Applied Physics,
Faculty of Science and Technology,
Universiti Kebangsaan Malaysia, 43600 UKM Bangi, Selangor, Malaysia
[2]School of Physics,
Universiti Sains Malaysia, 11800 Penang, Penang, Malaysia

[*]Corresponding author: naifalhardan@ukm.edu.my

Received: 31 January 2022; Accepted: 19 May 2022; Published: 27 December 2022

Abstract

This work describes the gas sensing performance of undoped zinc oxide (ZnO) and ZnO doped with 2 atomic% aluminum (ZnO: Al 2% at.) prepared via the thermal oxidation of zinc (Zn) and Al metal. The prepared films exhibited a polycrystalline structure of the hexagonal ZnO structure. The element composition shows the presence of Zn, O and Al, with Al percentage of approximately 2.2% at. The current-voltage characteristic was used to study the effect of the low hydrogen (H_2) concentrations on the sensing properties of ZnO and ZnO: Al. The maximum response of the undoped ZnO was approximately 100 at an operating temperature of 400 ℃ and increased to approximately 2000 at an operating temperature of 300 ℃ after doping with 2% at. Al. The current study reveals the promising potential for the Al-doped ZnO for low H_2 gas concentrations, as there was an enhancement in the response and reduction in the operating temperature of the doped ZnO with Al.

Keywords: hydrogen gas sensors, doping process, ZnO:Al

Abstrak

Kerja ini menerangkan prestasi penderiaan gas untuk zink oksida (ZnO) tanpa dop dan ZnO terdop 2 atom% aluminum (ZnO: Al 2% at.) yang disediakan melalui pengoksidaan terma logam zink (Zn) dan Al. Filem yang disediakan mempunyai struktur polikristal iaitu struktur heksagonal ZnO. Komposisi unsur menunjukkan kehadiran Zn, O dan Al, dengan peratusan Al pada anggaran 2.2% at. Ciri Arus-Voltan telah digunakan untuk mengkaji kesan kepekatan hidrogen (H_2) rendah terhadap sifat penderiaan ZnO dan ZnO:Al. Gerakbalas maksimum ZnO tanpa dop dalam anggaran 100 pada suhu operasi 400℃ dan meningkat kepada 2000 pada suhu operasi 300℃ setelah didop dengan Al. Kajian semasa menunjukkan ZnO terdop Al mempunyai potensi baik pada kepekatan gas H_2 yang rendah, di mana pengayaan dalam respons dan pengurangan dalam operasi suhu terhadap ZnO didop Bersama Al.

Kata kunci: hidrogen penderia gas, proses doping, ZnO:Al

Introduction

Recently, metal oxide semiconductor gas sensors have attracted considerable attention due to their applications in integrated circuit processes [1-3]. It is known that semiconductor sensors have been widely used and studied owing to their low cost, small size, and reliability [4-6]. However, the performance of the gas sensors based on metal oxide semiconductors showed drawbacks, as they need high operating temperatures and show a relatively low sensitivity.

The modification and the improvements in the metal oxide semiconductor gas sensors performance can be approached with different paths. Surface modification [7, 8] and doping process [9, 10] are among them. Recently, extensive studies on the doping process and its effect on the gas sensing performance of the metal oxide semiconductor were conducted. Elements such as chromium [10], indium [11], magnesium [12] aluminum (Al) [13-16] and others [17] have been carried out for different gas sensing applications. Aluminium was the most studied element for doping ZnO for several applications, such as conductive transparent layers [18]. In addition, the Al is inexpensive metal and abundant as compared with the other doped elements.

There are many published reports on the application of aluminum as a dopant for ZnO based gas sensors. Paraguay et al. [19] prepared ethanol vapor sensors based on ZnO, and different metals such as tin, indium, Al, iron and copper were used as dopants. No difference in operating temperature was observed. However, the ethanol vapor sensor based on ZnO doped with tin shows the highest sensitivity for ethanol vapor. Hijri et al. [13] prepared ZnO doped with 1-5% atomic Al nanoparticles via sol-gel process. The working operating temperature was in the range of 250-300 ^{o}C. The sensors based on ZnO: Al manifested a higher response than the undoped ZnO sensor in carbon monoxide environment. Zan et al. [20] synthesized ZnO: Al (0.1/0.075/0.05/0.025 mol/L) via a hydrothermal method. Different nanostructure morphologies were prepared, and the operating temperatures of the prepared ZnO: Al nanostructures were almost the same, despite the fact that different nanostructure morphologies were prepared. However, the sensitivity of the disk shape structures was the heights compared to other nanostructure morphologies. Several gases were demonstrated in the study, such as ammonia, carbon monoxide, and H_2. The chemical bath deposition method was conducted to prepare ethanol vapor sensors based on undoped ZnO and doped ZnO: Al. The optimum performance of the prepared sensor was for the sample with Al concentration equal to 2.90 at% [21]. The prepared ethanol sensor was operated at 300^{o}C as a working temperature. Furthermore, Yoo et. al [16] reported on the sensing of acetone by Al-doped ZnO for breath analysis applications. It was reported that doping ZnO with 1 at% Al will enhance the detection performance of the ZnO nanoparticles.

Hydrogen is one of the most gasses demonstrated for their importance as one of the resources of clean energy [22, 23]. H_2 gas is considered as one of the flammable gasses with a wide range of flammability in the air, which is about 4–75% by volume. The lowest limit of H_2 concentration in the atmosphere to cause an explosion is 4.65%, making it one of the most flammable gasses [24]. Sensors with the ability to detect low levels of H_2 ranging from 0.1 ppm to 100 ppm are required for applications involving leak detection in hydrogen fuel systems [23, 25].

Currently, there are few studies regarding the gas sensing properties of ZnO films prepared by oxidation as well as the process of doping it. Furthermore, the effect of the applied bias voltage on the gas sensing performance of the undoped and doped ZnO:Al was not explored wildly. In this study, we prepared zinc oxide (ZnO) and aluminum doped zinc oxide (ZnO: Al) through the thermal oxidation of dc sputtered Zn metal. The aim of this study is to enhance the sensing properties of the ZnO gas sensor through the doping process for H_2 gas sensors.

Materials and Methods

Silicon n-type wafer with (1 0 0) orientation was used as a substrate. Initially, the cleaning process of the wafer is

according to the RCA (Radio Corporation of America) method [26]. A silicon dioxide (SiO_2) thick layer is grown through a thermal oxidation process. Platinum (Pt) is used as a heating element and electrode. The pattern of the heating element and electrodes was carried out using the photolithography technique. Zn metal and Zn + Al thin films were coated using the A306 dc sputtering unit from Edwards. The target was high purity Zn metal target with a purity of >99.99% (diameter 7.62 cm) from (Xiamen Advanced and High-tech Material Co. Ltd, China) for the first batch of samples, while a high purity 2 cm Al rod (99.99% from Sigma-Aldrich (M) Sdn Bhd, Malaysia) with a diameter of 2 mm attached on top of the Zn target for the doped Zn. After reaching a pressure below 1 x 10^{-5} mbar, Ar gas was introduced into the chamber through a needle valve. During this process, the working pressure was held constant at approximately 4.5 x 10^{-2} mbar, and the dc power was maintained at 250 W.

The oxidation process was performed using a controlled tube furnace from Lenton. Both samples were inserted at room temperature, which was subsequently raised up to 400 ℃ at the rate of 5℃.min^{-1} with a constant flow rate of high purity (99.98%) oxygen. The oxidation time was 30 min. The film's color changed to white after the oxidation process. The thickness of the produced films was (300 ± 20) nm as measured by Filmetrics F20 optical reflectometer (based on the optical interference method). PANalytical X-ray diffractometer (HR-XRD) is used to obtain the crystal structure of the prepared films. The diffraction angles were in the range of 20° - 60°. A scanning electron microscope (SEM JEOL model JSM-6460 LV) with an energy dispersion spectroscopy (EDS type INCAx from OXFORD instrument) was used for structure, surface morphology, and elemental analysis of the prepared samples. Atomic force microscope (AFM) was also used for the morphology of the prepared samples' surface.

The current-voltage (I-V) characteristic of the sensor was measured using a programmable KEITHLEY Electrometer – model 617, which also supplied the voltage V ranging from -2 to 2 volts. A DC power supply was used for supplying the voltage to the heating element at the operating temperature between 50 ℃ to 450 ℃. A calibrated K - type thermocouple was mounted on the device to determine the operating temperature of the sensor. After 3 min of turning on the gas flow, the measurements were commenced to ensure a homogeneous distribution of the gas under study inside the chamber. The output current was collected as a function of different H_2 concentration (0-120) ppm. The test chamber was made of stainless steel, creating a volume of about 8200 cm^3. Highly grade 2% H_2 balanced in nitrogen (MOX-LINDE GASES SDN BHD, Malaysia) was used as a test gas. The measurements were taken at room temperature at humidity and temperature of 62% and 25℃, respectively.

Results and Discussion

Structure and elements analysis

The X-ray diffraction patterns of the 30-min thermal oxidation of Zn metal and Al-doped Zn are depicted in Figure 1. The pattern shows the polycrystalline nature of the prepared samples. Furthermore, there was no evidence of Zn metal in both prepared undoped and doped ZnO films, which confirmed the complete conversion of Zn metal to ZnO. The Bragg angles appear at 31.8°, 34.3°, 36.2°, and 56.8°, which belong to the (100), (002), (101) and (102) phases of ZnO (JCPDS card no. 36-1451), respectively. The decrease in the peak's intensity after doping with Al is also worth noting. This might be attributed to the existence of Al_2O_3 grains that interrupt the nucleation of the structure growth [27]. The EDX values for ZnO and ZnO: Al are shown in Table 1, along with their corresponding elemental compositions. It is clear that the Zn:O ratio is almost identical, and that the Al concentration is approximately 2.2at%.

Table 1. The element percentage of the ZnO and ZnO:Al samples prepared through the 30-minute thermal oxidation of Zn and Zn:Al

Elements	Atomic (%)	
	ZnO	ZnO: Al
O	52.48	52.17
Zn	47.52	45.65
Al	-	2.20

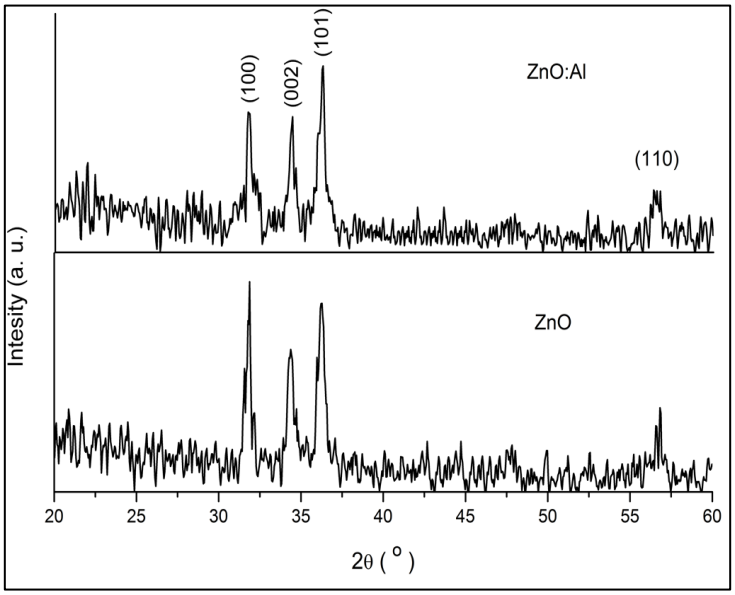

Figure 1. HR-XRD of ZnO and ZnO: Al samples after a 30-minute thermal oxidation at 400 ℃

The SEM and AFM micrographs of the surface of both sensors are depicted in Figure 2. It can be observed that the undoped ZnO surface appears to be more condensed as compared to the doped one, which demonstrated a porous microstructure with larger grains. The enhancement of the ZnO: Al grains size is due to the segregation of Al content into the grain boundaries [28]. The AFM micrograph also confirms that the doped ZnO possesses a rougher surface as compared to the undoped one. The root mean square of surface roughness measured by AFM for the undoped ZnO was 45 nm, which increased to 78 nm for the doped ZnO with 2.2at% Al. Surface roughness and less compact structure may be attributed to the migration of Al dopants towards the grain boundary, where they react with oxygen atoms and segregate as Al_2O_3 [29].

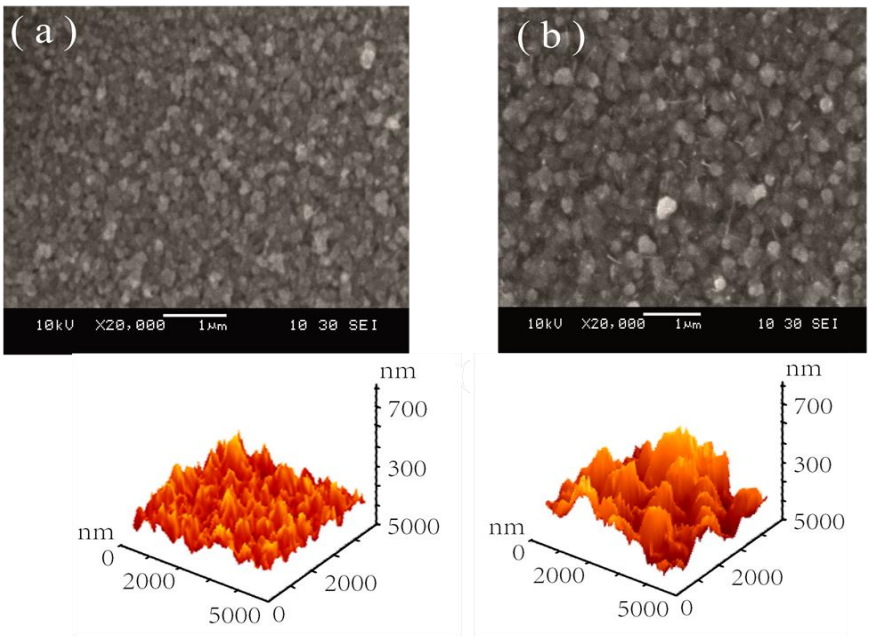

Figure 2. The SEM and AFM micrographs for both (a) ZnO and (b) ZnO: Al were prepared through the thermal oxidation of Zn metal; the bar length is 1 μm

The current-voltage characterization

The resistance of both prepared gas sensors samples in the temperature range starting from room temperature up to 450 ℃ is measured in an air atmosphere, and the results are shown in Figure 3. It is worth noting that the resistance of both sensing materials decreased along with the temperature. This indicates the semiconductor behavior of both prepared samples. Moreover, the resistance of the ZnO: Al was lower than that of undoped ZnO in the temperature range from 50 ℃ to around 250 ℃. The lower baseline resistance could be attributed to the higher charge carrier concentration resulting from the donor nature of the substitution of Al^{3+} on Zn^{2+} sites [28, 30]. These results are comparable with those published [13, 31]. The decrease in sheet resistance at 100-250 ℃ was due to the thermal excitation of electrons into the conduction band. Furthermore, it has been reported that undoped ZnO undergoes a reduction process as the temperature rises to form oxygen vacancies, which are immediately ionized to donate electrons to the conduction band [32, 33]. The next regime of the behavior (above 250℃) exhibited a positive temperature coefficient of resistance (PTCR) for the ZnO sample. However, for the ZnO: Al sample, PTCR appeared in the temperature ranging from 250 – 350 ℃ before giving way to the negative temperature coefficient (NTCR) of the resistance regime at temperatures above 350 ℃. The PTCR regime in the ZnO sample is probably due to the thermal desorption of the (OH^-) layer [34] or the adsorption of various oxygen molecules on the ZnO surface [30].

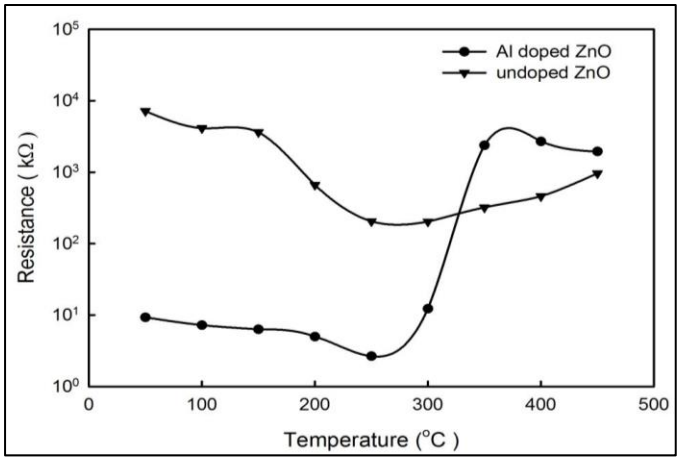

Figure 3. The electrical resistance behavior of the ZnO and ZnO: Al samples

In order to evaluate the quality of the manufactured sensors as well as determine the optimum operating temperature, both sensors were exposed to a fixed concentration of H_2 (100 ppm), while the temperature was varied between 100℃ and 450℃ with a step of 50℃ (there was the insignificant response at temperature lower than 100℃ for both samples). The quality levels of both ZnO and ZnO: Al sensors were estimated by measuring their response (Equation 1), which can be calculated by the ratio of the resistance in the air (Ra) and resistance in the hydrogen gas atmosphere (R_g) [34]:

$$S = \frac{Ra}{Rg} \quad (1)$$

Figure 4 (semi-log graph) reveals the response of both prepared sensors as a function of the operating temperatures. In both cases, the response to the 100 ppm H_2 was increased with the temperature. The maximum response of the undoped ZnO was approximately 100 and occurred at 400℃, and it was approximately 2100 at an operating temperature of 300℃ for the doped ZnO:Al gas sensors. It is, therefore, concluded that the optimum operating temperature is 400℃ and 300 ℃ for the undoped ZnO and doped ZnO:Al gas sensors, respectively.

The reaction rate between the gas under test with the surface absorbed oxygen species is low at low operating temperatures. This is probably due to the high activation energy barrier of the surface reaction. Increasing the operating temperature will enhance the sensor response, which probably is due to the sufficient thermal energy to overcome the barrier height. According to Krishnakumar et al. [35], Patil and Patil [36] and Barreca et al. [8], the adsorbed oxygen may desorb from the surface at higher temperatures (the adsorbed oxygen will not be enough to react with the gas). This will result in decreasing the gas response at higher temperatures. It is obvious that the ZnO: Al sensor has a much lower operating temperature and higher response than that of the undoped ZnO sensor.

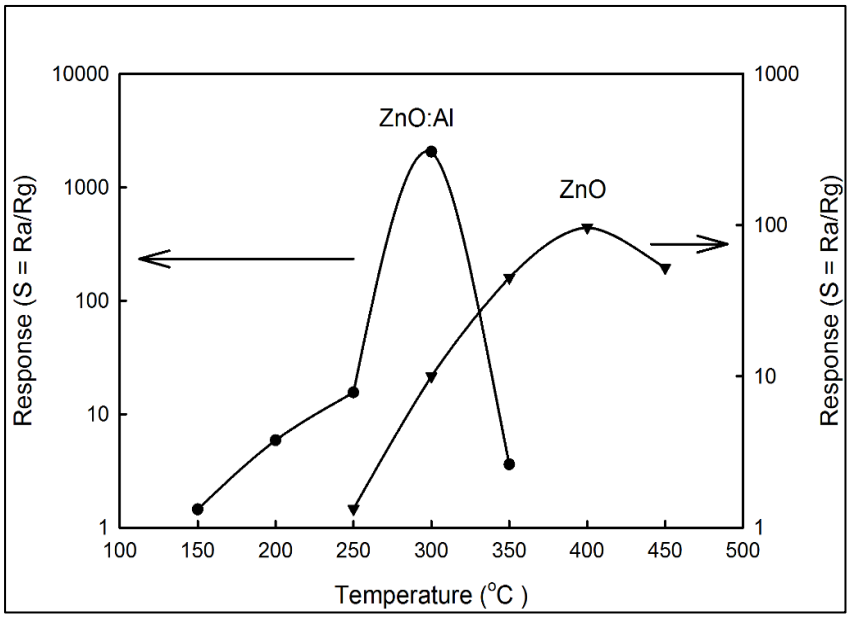

Figure 4. The operating temperature of the ZnO: Al and ZnO gas sensors.

We believe that the enhancement of the gas response at lower operating temperatures is due to the incorporation of the Al metal. Consequently, the surface activity is enhanced as Al has lower ionization energy than the Zn [10]. Furthermore, the modification in the surface nature may consider another factor that might enhance the response of the doped ZnO gas sensor. The increase in the roughness of the surface will result in an increase in the surface to volume ratio, which will allow the gas to penetrate more through the sensitive area of the oxide. On the other hand, the surface is usually dense for the undoped ZnO, and the sensing reactions are restricted to the surface.

Several authors [37, 38] have observed the occurrence of shifting operating temperature by doping; it was found that such an effect is related to the changes in the reaction equilibrium, which strongly depend on operating temperature [38]. Figure 5 shows the current-voltage characteristic of both the undoped and doped ZnO with 2% at. Al in H_2 atmosphere with the concentration ranging from 40 to 160 ppm. The operating temperatures were fixed at 400 ^oC and 300 ^oC for the undoped and doped ZnO, respectively. The figure shows that the current magnitude for both sensors increased as the gas concentrations increased. Furthermore, the current values of the doped ZnO are becoming higher than the undoped ZnO.

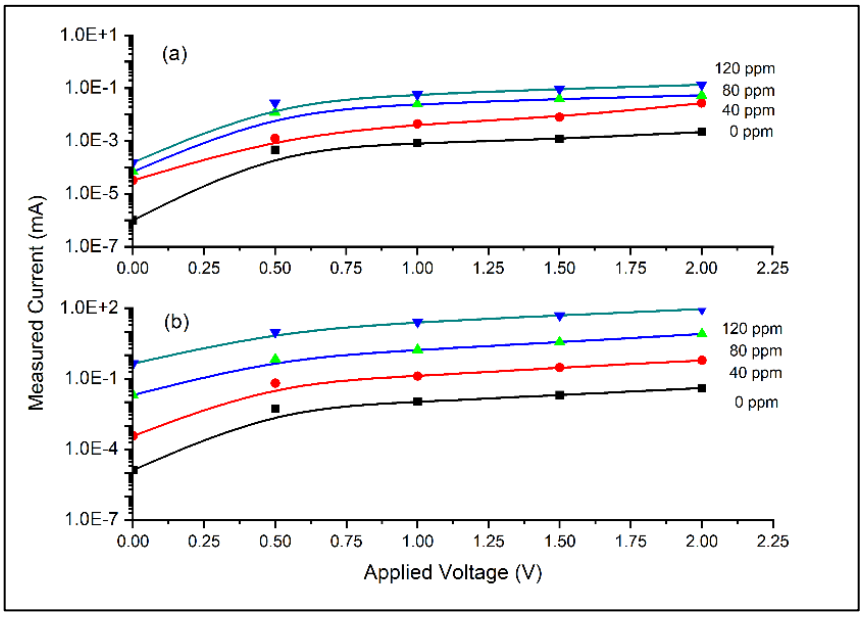

Figure 5. The I-V characteristic of (a) ZnO and (b) ZnO: Al in the H_2 atmosphere with concentration ranging from 40 to 160 ppm

It is well accepted that the detection of reduction gases over the metal oxide surface involves an adsorption−oxidation−desorption process [39]. Here, the oxygen molecules play an important role in this process. Upon the exposure of the metal oxide in the air at elevated temperatures (higher than 200℃, oxygen molecules are adsorbed over at surface of the oxide, and the formation of oxygen ions (O^-, O^{2-} or O^{-2}) will accrue (Equation 2-5), by attracting electrons from the conduction band of the metal oxide. The reaction can be summarized as follow [37];

$$O_2(gas) \Leftrightarrow O_2(adsorbed) \quad (2)$$

$$O_2(ads) + \bar{e} \Leftrightarrow O_2^-(ads) \quad (3)$$

$$O_2^-(ads) + \bar{e} \Leftrightarrow 2O^-(ads) \quad (4)$$

$$O^-(ads) + \bar{e} \Leftrightarrow O^{-2}(ads) \quad (5)$$

This will form a space-charge depletion layer on the surface of the oxide resulting in a reduction of the carrier concentration. When the sensors are exposed to a reducing gas (in this case is H_2), the H_2 gas reacts with the adsorbed oxygen ions on the sensor's surface, and as a result, the electrons will be released back into the conduction band, causing an increase in the produced current, as can be expected (Equation 6) from the following reaction between the hydrogen gas molecules and the adsorbed oxygen:

$$H_2 + O^- \rightarrow H_2O(gas) + e^- \quad (6)$$

As the doping content of Al increases the carrier concentration, this will result in a higher output current as compared to the undoped ZnO gas sensor. The behavior of both undoped ZnO and doped ZnO:Al with the H_2 concentrations from (0 - 120) ppm at a bias voltage of 2V is depicted in Figure 6. It can be observed

that the sensor's measured current increased when exposed to hydrogen up to 120 ppm with a good linearity that proves the suitability of using the ZnO for low hydrogen concentrations.

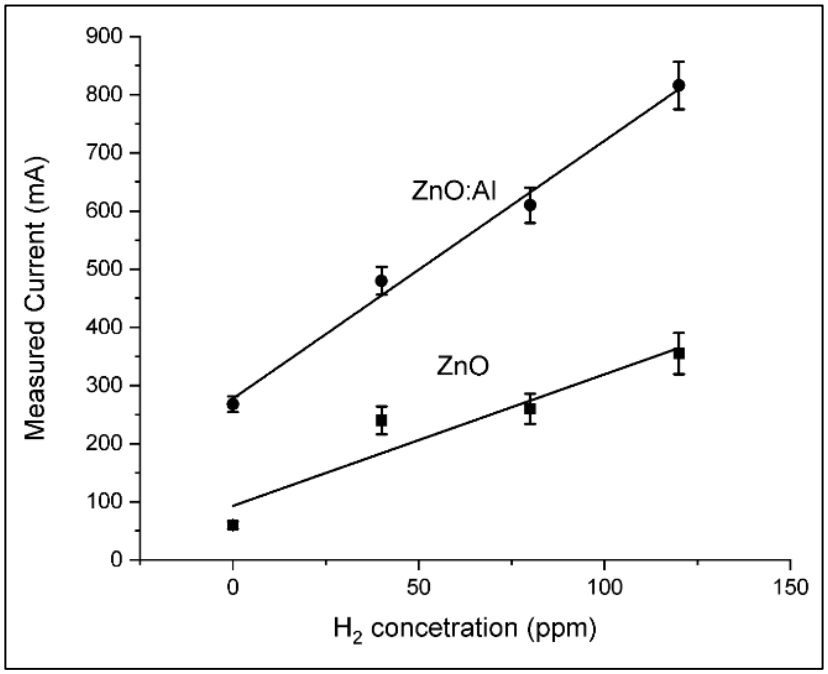

Figure 6. The response of the measured current for ZnO and ZnO: Al when exposed to the H2 atmosphere for different concentration levels. The operating temperature of the undoped and doped ZnO was 400 ℃ and 300 ℃, respectively, and the applied voltage was fixed at 2V

Conclusion

In this study, undoped ZnO and doped ZnO: Al gas sensors were successfully prepared by the thermal oxidation of the Zn metal at 400℃. It was also found that the operating temperature was reduced, and the sensitivity was higher for the doped ZnO: Al sensor. The I – V characteristic of both samples show a significant response for the measured H_2 concentration range. Due to the increase in the carrier concentration of the Al doped ZnO, the enhancement of response was noticed. The results show a potential application of the Al doped ZnO for low range H_2 concentration gas sensors.

Acknowledgement

The authors acknowledge the financial support of CRIM- Universiti Kebangsaan Malaysia (UKM), grant GGPM-2020-047. The authors also acknowledged the support of the school of physics Universiti Sains Malaysia (USM).

References

1. Müller, G., Friedberger, A., Kreisl, P., Ahlers, S., Schulz, O. and Becker, T. (2003). A MEMS toolkit for metal-oxide-based gas sensing systems. *Thin Solid Films*, 436(1): 34-45.
2. Tuller, H. L. and Mlcak, R. (2000). Advanced sensor technology based on oxide thin film-MEMS integration. *Journal of Electroceramics*, 4(2): 415-425.
3. Graf, M., Barrettino, D., Zimmermann, M., Hierlemann, A., Baltes, H., Hahn, S., ... and Weimar, U. (2004). CMOS monolithic metal-oxide sensor system comprising a microhotplate and associated circuitry. *IEEE Sensors Journal*, 4(1): 9-16.

4. Alenezi, M. R., Henley, S. J., Emerson, N. G. and Silva, S. R. P. (2014). From 1D and 2D ZnO nanostructures to 3D hierarchical structures with enhanced gas sensing properties. *Nanoscale,* 6(1): 235-247.
5. Al-Hardan, N. H., Abdul Hamid, M. A., Shamsudin, R., Othman, N. K. and Kar Keng, L. (2016). Amperometric non-enzymatic hydrogen peroxide sensor based on aligned zinc oxide nanorods. *Sensors*, 16(7): 1004.
6. Al-Khalqi, E. M., Hamid, M. A. A., Shamsudin, R., Al-Hardan, N. H., Jalar, A. and Keng, L. K. (2020). Zinc oxide nanorod electrolyte–insulator–semiconductor sensor for enhanced 2-methoxyethanol selectivity. *IEEE Sensors Journal*, 21(5): 6234-6240.
7. Law, J. B. K. and Thong, J. T. L. (2008). Improving the NH_3 gas sensitivity of ZnO nanowire sensors by reducing the carrier concentration. *Nanotechnology*, *19*(20), 205502.
8. Barreca, D., Bekermann, D., Comini, E., Devi, A., Fischer, R. A., Gasparotto, A., ... and Tondello, E. (2010). 1D ZnO nano-assemblies by Plasma-CVD as chemical sensors for flammable and toxic gases. *Sensors and Actuators B: Chemical*, 149(1): 1-7.
9. Basu, S. and Basu, P. K. (2009). Nanocrystalline metal oxides for methane sensors: role of noble metals. *Journal of Sensors,* 2009: 861968.
10. Al-Hardan, N. H., Abdullah, M. J. and Aziz, A. A. (2013). Performance of Cr-doped ZnO for acetone sensing. *Applied Surface Science,* 270: 480-485.
11. Hjiri, M., Dhahri, R., Omri, K., El Mir, L., Leonardi, S. G., Donato, N. and Neri, G. (2014). Effect of indium doping on ZnO based-gas sensor for CO. *Materials Science in Semiconductor Processing*, 27: 319-325.
12. Al-Khalqi, E. M., Abdul Hamid, M. A., Al-Hardan, N. H. and Keng, L. K. (2021). Highly sensitive magnesium-doped ZnO nanorod pH sensors based on electrolyte–insulator–semiconductor (EIS) sensors. *Sensors*, 21(6): 2110.
13. Hjiri, M., El Mir, L., Leonardi, S. G., Pistone, A., Mavilia, L. and Neri, G. (2014). Al-doped ZnO for highly sensitive CO gas sensors. *Sensors and Actuators B: Chemical*, 196: 413-420.
14. Yang, Z., Huang, Y., Chen, G., Guo, Z., Cheng, S. and Huang, S. (2009). Ethanol gas sensor based on Al-doped ZnO nanomaterial with many gas diffusing channels. *Sensors and Actuators B: Chemical*, 140(2): 549-556.
15. Navale, S. C., Ravi, V., Mulla, I. S., Gosavi, S. W. and Kulkarni, S. K. (2007). Low temperature synthesis and NOx sensing properties of nanostructured Al-doped ZnO. *Sensors and Actuators B: Chemical*, 126(2): 382-386.
16. Yoo, R., Güntner, A. T., Park, Y., Rim, H. J., Lee, H. S. and Lee, W. (2019). Sensing of acetone by Al-doped ZnO. *Sensors and Actuators B: Chemical*, 283: 107-115.
17. Darvishnejad, M. H., Firooz, A. A., Beheshtian, J. and Khodadadi, A. A. (2016). Highly sensitive and selective ethanol and acetone gas sensors by adding some dopants (Mn, Fe, Co, Ni) onto hexagonal ZnO plates. *RSC Advances*, 6(10): 7838-7845.
18. Lee, S. H., Han, S. H., Jung, H. S., Shin, H., Lee, J., Noh, J. H., ... and Shin, H. (2010). Al-doped ZnO thin film: a new transparent conducting layer for ZnO nanowire-based dye-sensitized solar cells. *The Journal of Physical Chemistry C*, 114(15): 7185-7189.
19. Miki-Yoshida, M., Morales, J. and Solis, J. (2000). Influence of Al, In, Cu, Fe and Sn dopants on the response of thin film ZnO gas sensor to ethanol vapour. *Thin Solid Films*, 373(1-2): 137-140.
20. Zan, L., Wei, Q. and Xiaohong, W. (2015). Controllable hydrothermal synthesis of Al-doped ZnO with different microstructures, growth mechanisms, and gas sensing properties. *RSC Advances,* 5(69): 56325-56332.
21. Yuliarto, B., Nulhakim, L., Ramadhani, M. F., Iqbal, M. and Nuruddin, A. (2015). Improved performances of ethanol sensor fabricated on Al-doped ZnO nanosheet thin films. *IEEE Sensors Journal,* 15(7): 4114-4120.
22. Fardindoost, S., Rahimi, F. and Ghasempour, R. (2010). Pd doped WO_3 films prepared by sol–gel process for hydrogen sensing. *International Journal of Hydrogen Energy,* 35(2): 854-860.

23. Grimes, C. A., Ong, K. G., Varghese, O. K., Yang, X., Mor, G., Paulose, M., ... and Mason, A. J. (2003). A sentinel sensor network for hydrogen sensing. *Sensors*, 3(3): 69-82.
24. Al-Salman, H. S., Abdullah, M. J. and Al-Hardan, N. (2013). ZnO thin film nanostructures for hydrogen gas sensing applications. *Ceramics International,* 39: S447-S450.
25. Boon-Brett, L., Bousek, J., Black, G., Moretto, P., Castello, P., Hübert, T. and Banach, U. (2010). Identifying performance gaps in hydrogen safety sensor technology for automotive and stationary applications. *International Journal of Hydrogen Energy*, 35(1): 373-384.
26. Kern, W. (1990). The evolution of silicon wafer cleaning technology. *Journal of the Electrochemical Society,* 137(6): 1887.
27. Jeong, S. H., Kho, S., Jung, D., Lee, S. B. and Boo, J. H. (2003). Deposition of aluminum-doped zinc oxide films by RF magnetron sputtering and study of their surface characteristics. *Surface and Coatings Technology,* 174: 187-192.
28. Ma, T. Y. and Lee, S. C. (2000). Effects of aluminum content and substrate temperature on the structural and electrical properties of aluminum-doped ZnO films prepared by ultrasonic spray pyrolysis. *Journal of Materials Science: Materials in Electronics,* 11(4): 305-309.
29. Lupan, O., Shishiyanu, S., Ursaki, V., Khallaf, H., Chow, L., Shishiyanu, T., ... and Railean, S. (2009). Synthesis of nanostructured Al-doped zinc oxide films on Si for solar cells applications. *Solar Energy Materials and Solar Cells,* 93(8), 1417-1422.
30. Haug, F. J., Geller, Z., Zogg, H., Tiwari, A. N., & Vignali, C. (2001). Influence of deposition conditions on the thermal stability of ZnO: Al films grown by rf magnetron sputtering. *Journal of Vacuum Science & Technology A: Vacuum, Surfaces, and Films,* 19(1): 171-174.
31. Sahay, P. P. and Nath, R. K. (2008). Al-doped ZnO thin films as methanol sensors. *Sensors and Actuators B: Chemical,* 134(2), 654-659.
32. Gurlo, A. and Riedel, R. (2007). In situ and operando spectroscopy for assessing mechanisms of gas sensing. *Angewandte Chemie International Edition,* 46(21): 3826-3848.
33. Nenov, T. G. and Yordanov, S. P. (2020). Ceramic sensors: technology and applications. CRC press.
34. Moseley, P. T. (1997). Solid state gas sensors. *Measurement Science And Technology,* 8(3): 223.
35. Krishnakumar, T., Jayaprakash, R., Pinna, N., Donato, N., Bonavita, A., Micali, G. and Neri, G. (2009). CO gas sensing of ZnO nanostructures synthesized by an assisted microwave wet chemical route. *Sensors and Actuators B: Chemical,* 143(1): 198-204.
36. Patil, D. R. and Patil, L. A. (2009). Cr_2O_3-modified ZnO thick film resistors as LPG sensors. *Talanta,* 77(4): 1409-1414.
37. Xia, H., Wang, Y., Kong, F., Wang, S., Zhu, B., Guo, X., ... and Wu, S. (2008). Au-doped WO_3-based sensor for NO2 detection at low operating temperature. *Sensors and Actuators B: Chemical,* 134(1), 133-139.
38. Ferro, R., Rodriguez, J. A. and Bertrand, P. (2005). Development and characterization of a sprayed ZnO thin film‐based NO_2 sensor. *Physica Status Solidi* (C), 2(10): 3754-3757.
39. Tian, S., Yang, F., Zeng, D. and Xie, C. (2012). Solution-processed gas sensors based on ZnO nanorods array with an exposed (0001) facet for enhanced gas-sensing properties. *The Journal of Physical Chemistry C,* 116(19): 10586-10591.